

Shockley and Tamm surface states in photonic crystals

N. Malkova* and C. Z. Ning†

Center for Nanotechnology, NASA Ames Research Center, Moffett Field, California 94035, USA

(Received 17 February 2006; published 27 March 2006)

Existence of the Shockley surface states in photonic crystals is demonstrated for the first time. We show that in photonic crystals, the surface states of defect chain with unit cell containing one defect are the Tamm rather than Shockley states as commonly assumed. The Shockley states can appear only in the defect chain with unit cell containing more than one defect. We first analyze the surface states using the tight-binding theory. Theoretical predictions are confirmed by the numerical simulations.

DOI: 10.1103/PhysRevB.73.113113

PACS number(s): 78.68.+m, 42.70.Qs, 42.79.Gn, 73.20.At

There is a great deal of interest in the surface excitations supported by a periodical array of the dielectric materials or photonic crystals (PC). Such surface waves are called surface Bloch waves (SBW).¹ The SBWs appear to be superior alternatives in many applications to another surface excitations called surface plasmon polaritons.² First of all, the properties of PC can be engineered to allow for the SBW at virtually any optical frequency. Second, the low loss of the dielectric PCs may enhance the surface sensitivity.³ The SBWs were demonstrated experimentally and theoretically both in one dimensional^{1,4,5} and in multi-dimensional⁶⁻⁹ PCs. It has been shown recently that, similar to surface plasmon on corrugated metal film,¹⁰ the SBWs on PCs can cause highly directional emission from the PC waveguide.¹¹ This effect holds promise for application of the SBWs in subwavelength devices.

Surface states in solids can be either Tamm states¹² or Shockley states.¹³ The Tamm surface states for electrons are the direct consequence of the strong perturbation at a solid surface, resulting in an asymmetric potential about the surface, or asymmetric termination of periodical potential.¹² They appear as soon as an asymmetry parameter becomes comparable to the coupling constant β between the nearest neighbors in the lattice. Since the coupling constant β determines the width of the allowed band directly, the Tamm states are more likely to occur for narrow-band materials with large interatomic distance.¹² The situation is quite different for the Shockley surface states which appear when atoms are close to each other and interact strongly.¹³ The Shockley states do not require existence of an asymmetric potential at the surface and they emerge from the so-called crossing bands.¹³ Attempts were made to extend such analogies to PCs.^{1,14} In studying multilayer structures, Yeh and Yariv^{1,5} identified SBWs in this one-dimensional PCs as analogous to the Shockley surface states in solids. However the authors could not reconcile this analogy with the fact that the surface electromagnetic wave can appear inside the band gap only when the separation between the identical layers (waveguides) is large enough. While the key condition for the Shockley surface states in solids is that the interatomic distance becomes small enough such that the allowed energy bands involved¹³ cross. In spite of this basic difference, the idea of similarity between the SBWs in PCs and the Shockley states in solids has been widely accepted.¹⁴

The goal of this paper is twofold. First we show that the surface states in PCs with a basis of one dielectric rod

(simple unit cell), are *not* the Shockley states as commonly assumed, but rather the Tamm states. Second we demonstrate a new type of the surface excitation in PCs which is analogous to the Shockley surface states. We show that the Shockley surface states can appear in a PC with a complex basis of at least two rods (complex unit cell). The unit cell should contain either alternating dielectric rods supporting the *s*- and *p*-modes or/and alternating strong and weak bonds. We first investigate both types of the surface states in these structures theoretically using the empirical tight-binding model. Our theoretical predictions are then confirmed by the finite difference time domain (FDTD) simulations. As model systems we consider structures shown in Fig. 1. They are periodic arrays of the infinitely long dielectric rods embedded in another dielectric medium. These otherwise perfect two-dimensional PCs are doped with a chain of the defect rods separated by d . Structure 1 in Fig. 1(a) consists of single-defect unit cells and corresponds to the situation commonly studied for surface states in PCs.^{1,6,14} Structures 2 [Fig. 1(b)]

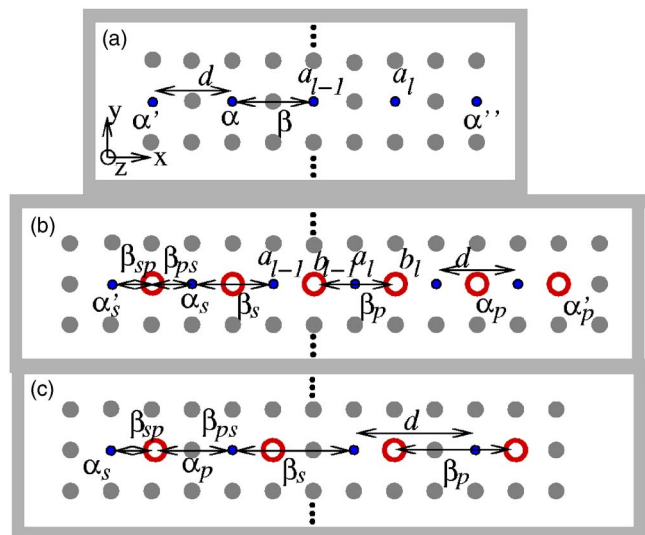


FIG. 1. (Color online) Coupled-defect structures including *s*-defects (small filled circles) and *p*-defects (open large circles) embedded in a host PC (gray circles): (a) Structure 1 with unit cell containing one *s*-defect; (b) Structure 2 with equivalent bonds between the *s*- and *p*-defects with 6 complete unit cells; (c) Structure 3 with alternating strong (short) and weak (long) bonds and 4 complete unit cells.

and 3 [Fig. 1(c)] consist of complex unit cells with two different defects connected by either equivalent bonds [Fig. 1(b)] or alternating strong (short) and weak (long) bonds [Fig. 1(c)]. We assume that one of the defects supports the nondegenerate s -mode and the other—the double-degenerate p -mode. In order to simplify the analysis we design these structures in such a way that the defect states (or the allowed band of the chain) fall inside the band gap of the host crystal. Then at the first order approximation we neglect the coupling between the defect rods and the host crystal. Therefore, we can consider these structures as periodical chains installed in another quasi-homogeneous medium.

In the framework of the tight-binding model,¹⁶ the wave function of the defect chain with complex unit cell (Fig. 1) is represented as a linear combination of the s -type, $\phi_s(r-nd)$, and two double degenerate p -type, $\phi_{px(y)}(r-md)$, eigenfunctions of the individual defects located at the n th and m th sites, respectively, $\Psi(r,t) = \sum_n a_n(t) \phi_s(r-nd) + \sum_{m,i=x,y} b_m^i(t) \phi_{pi}(r-md)$. The consistent description of this structure should include the coupling matrix elements between the nearest s -modes, β_s , and the p -modes, β_p , along with the coupling matrix elements between the nearest s -mode and p_x -mode, β_{sp} , and between the p_x - and s -defects, β_{ps} (see Fig. 1). By symmetry, the coupling between the s - and p_y -modes vanishes. Therefore, for our problem we can consider both defects as singlet mode s - and p -defects, and the x - and y -indexes will be dropped from now on. The coupling matrix elements $\beta_s(\beta_p)$ define the width of the allowed bands for the simple chains including only the equidistant s - or p -defect. While the matrix elements β_{sp} and β_{ps} describe the interaction between the s - and p -defects. The dynamics of the field amplitudes $a_l(t)$ and $b_l(t)$ in the l th unit cell is described by the following equations

$$i \frac{d}{dt} a_l = \alpha_s a_l + \beta_s (a_{l-1} + a_{l+1}) + \beta_{sp} b_l + \beta_{ps} b_{l-1},$$

$$i \frac{d}{dt} b_l = \alpha_p b_l + \beta_p (b_{l-1} + b_{l+1}) + \beta_{sp} a_l + \beta_{ps} a_{l+1}, \quad (1)$$

where $\alpha_{s,p} = \omega_{s,p} - i\gamma_{s,p}$ are the complex eigenvalues of the individual s - or p -defect. The coupling matrix elements are determined by the overlap integrals between the relevant defect modes.¹⁶ For a infinite chain, the solution of the problem is given by the dispersion relation:

$$\omega_{1,2}(k) = 1/2 [\alpha_s + \alpha_p + 2(\beta_s + \beta_p)c] \pm 1/2 \sqrt{[\alpha_s - \alpha_p + 2c(\beta_s - \beta_p)]^2 + 4\tilde{\beta}_{sp}^2}, \quad (2)$$

where $\tilde{\beta}_{sp}^2 = \beta_{sp}^2 + \beta_{ps}^2 + 2\beta_{sp}\beta_{ps}c$ and $c = \cos(kd)$. In the case of a finite chain with N unit cells we have $2N-2$ evolution equations from (1), with 2 boundary conditions:

$$i \frac{d}{dt} a_1 = \alpha'_s a_1 + \beta_{sp} b_2, \quad i \frac{d}{dt} b_N = \alpha'_p b_N + \beta'_{sp} a_N, \quad (3)$$

where α'_s , α'_p , and β'_s , β'_p , β'_{sp} are the eigenvalues and coupling constants of the end defects, respectively.

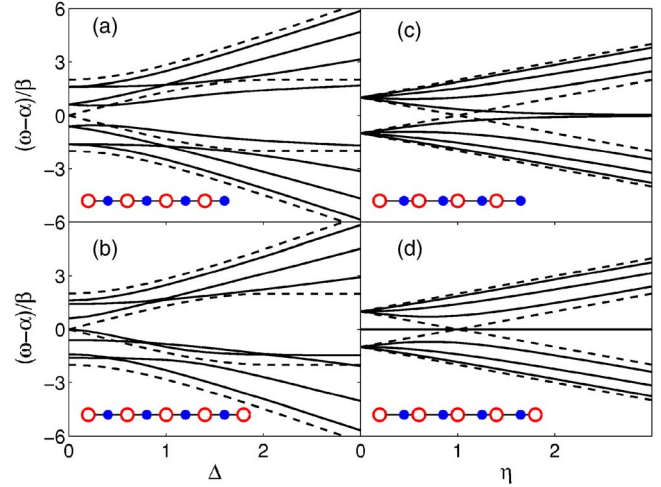


FIG. 2. (Color online) Energy spectrum of the defect chain with unit cell containing double defects with complete (a) and (c) and incomplete unit cells (b) and (d) for structures 2 (a) and (b) and structures 3(c) and (d). Insets illustrate the structures studied. Dashed lines show the boundaries of the allowed bands.

Equations (1) and (3) form the basis for the surface state problem of a one-dimensional system. The Tamm surface states immediately follow from the set, if we neglect the s - p hybridization.¹⁷ Then two surface states will emerge from the allowed band into the forbidden band if the asymmetry parameters satisfy $|\alpha_{s,p} - \alpha'_{s,p}| / \beta_{s,p} > 1$.¹⁵ Since coupling constant $\beta_{s,p}$ determines the width of the allowed band directly, the Tamm states are more likely to occur in the case of narrow band corresponding to large interatomic distance. On the other hand, the Shockley states do not require such asymmetry at surface and appear due to the termination of the s - p hybridized chain.¹⁵ To focus on the Shockley states only, we assume no asymmetric perturbation at the ends by setting $\alpha'_{s,p} = \alpha_{s,p}$ and $\beta'_{sp,s,p} = \beta_{sp,s,p}$.

We analyze now the Shockley problem for structures 2 and 3. Structure 2 in Fig. 1(b) is characterized by two identical bonds, or $\beta_{sp} = -\beta_{ps}$, and, by symmetry, $\beta_s \beta_p < 0$. To simplify the analysis we assume that $\alpha_s = \alpha_p = \alpha$ and $\beta_s = -\beta_p = \beta$. The energy spectrum of Eqs. (1) and (3) are shown in terms of $(\omega - \alpha) / \beta$ in Fig. 2 for 4 complete [Fig. 2(a)] and 5 incomplete unit cells [Fig. 2(b)] as function of the normalized coupling parameter $\Delta = |\beta_{sp} / \beta|$. The dashed lines show the edges of the allowed bands calculated from Eq. (2). We can see that, when a critical value of Δ is reached, the two states fall inside the inverted band gap. They become the surface modes localized at the surface and described by a complex wave vector. For the chain with integer number of complete unit cells, the surface modes are close to the two band-edges of the crossing bands [Fig. 2(a)]. While in the case of the incomplete unit cells, the surface modes appear only near one band-edge [Fig. 2(b)].

Structure 3 [Fig. 1(c)] provides another example of the Shockley states.¹⁵ For the sake of simplicity, we neglect the next nearest coupling, $\beta_s = \beta_p = 0$, and assume that $\alpha_s = \alpha_p = \alpha$. The energy spectrum in unit of $(\omega - \alpha) / \beta_{sp}$ is plotted against the ratio of the two coupling parameters $\eta = |\beta_{ps} / \beta_{sp}|$ for 4 complete [Fig. 2(c)] and 5 incomplete unit

cells [Fig. 2(d)]. First we analyze the structure with integer number of unit cells. If $\eta=0$ ($\beta_{ps}=0$), then the spectrum consists of 2 fourfold degenerate levels $\omega_{1,2}=\alpha\pm\beta_{sp}$. When $\eta>0$, the degeneracy is removed, resulting in 2 bands separated by the direct band gap. For $\eta=1$ (or $|\beta_{sp}|=|\beta_{ps}|$), the chain becomes the same as structure 2 with equivalent bonds and the two bands cross. When $\eta>1$, an inverted band gap is opened. At the same time, two states emerge from the allowed bands and move to the middle of the inverted band gap [Fig. 2(c)], generating two surface modes. From this analysis we can conclude that, in the structure with non-equivalent bonds, the surface states appear only at $\eta>1$, that is, only if the surfaces break the strong bonds. [Note from Fig. 1(c) β_{ps} bond is broken at surfaces.] We will not see the surface state in the opposite case if the two surfaces break the two weak bonds when $\eta<1$ [Fig. 1(c)]. A direct consequence of this effect is that in the structures with incomplete number of unit cells one surface mode exists for any values of the parameter η . The termination of such a structure implies that one of the surfaces must break the strong bond [see inset in Fig. 2(d)]. This necessarily gives rise to one surface mode at $\omega=\alpha$ [Fig. 2(d)].

To confirm the results of theoretical analysis, we perform a numerical simulation using the FDTD technique. Our computational domain are shown in Fig. 1 with perfectly matched layer boundary conditions. The PC structures are square lattice of the silicon rods ($\epsilon_r=11.9$) in vacuum ($\epsilon_o=1$). The main requirement for structure 1 to demonstrate the Tamm surface states is a large asymmetry parameter ($|\alpha'-\alpha|$). It can be shown that the eigenvalues (α' 's) of defects depend on their distance to surface.¹⁷ The eigenvalue of a defect decreases drastically when the defect is moved towards the surface. This effect can be used to control the asymmetry parameter, and thus the absence or existence of the Tamm surface states. Our analysis showed that the conditions of the Tamm states can be realized with regular rods of radius $R=0.35a$ and defect rods of $R_d=0.2a$, where a is the lattice constant. Such a defect creates the s -mode almost in the middle of the first band gap of TM mode (magnetic field in the plane). The defects are right at the surfaces as shown in Fig. 1(a) to have a large asymmetry parameter. To demonstrate the Shockley states in structures 2 and 3, we choose the host crystal with rods of radius $R=0.2a$ which has a TM bandgap of $\tilde{\omega}=\omega a/2\pi c=[0.28,0.48]$. The two defects supporting the s - and p -modes are rods of radius $R_{d1}=0.06a$ and $R_{d2}=0.3a$, respectively. These defects have almost the same eigenvalues $\tilde{\omega}=0.358$, which are close to the middle of the band gap. Thus, the coupling between host crystal bands and the defect chain can be ignored for these structures. To focus on the Shockley surface states only, we add one extra layer of the host crystal in structures 2 and 3 in Figs. 1(b) and 1(c) to avoid having no-zero asymmetry parameter.

The transmission coefficients calculated from the FDTD simulations and the field pattern for structure 1 with different defect separations are presented in Fig. 3(a). In agreement with Tamm's theory,¹⁵ the surface mode moves deeper inside the band gap, and becomes more strongly localized to the surface, the larger the distance between the defects (or the smaller the allowed band) [compare Fig. 3(b) and Fig. 3(c)].

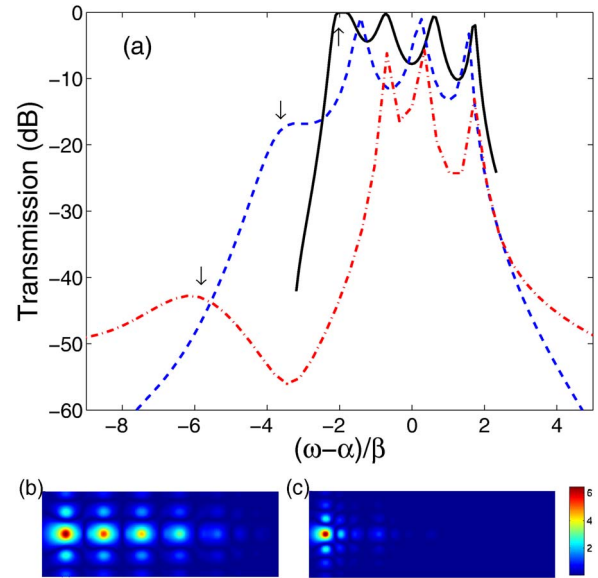


FIG. 3. (Color online) (a) Calculated transmission coefficient for structure 1 with defect separation $d=2a$ (solid line), $3a$ (dashed line), and $4a$ (dash-dotted line). The arrows point to the surface modes; The field pattern with defects separated by $2a$ (b) and $4a$ (c) at the resonance frequencies indicated by the arrow.

Our analysis also showed that the surface states disappear when the asymmetry parameter decreases, such as $|\alpha'-\alpha|<\beta$. We conclude that the surface states in PCs such as structure 1 with a single-defect unit cell are the direct consequence of the asymmetric termination of the periodic potential at the surface, $\alpha', \alpha'' \neq \alpha$. These features are typical of the Tamm states, rather than of the Shockley states in solids contrary to what was assumed in previous papers.^{1,14}

The results of our analysis for structures 2 and 3 are summarized in Fig. 4. The transmission coefficient and the dispersion relation for structure 2 are shown in Fig. 4(a) and 4(b). In agreement with the theoretical prediction of Fig. 2(a), we can clearly see the opening of the inverted band gap and the two surface modes indicated by arrows in Fig. 4(a). The distributions of the z component of the electric field for these modes are shown in Figs. 4(c) and 4(d). One of the surface modes splits off from the s -band [Fig. 4(c)] and another—from the p -band [Fig. 4(d)]. Both modes are not strongly localized to the surface since they lie close to the band-edges. Our detail analysis showed that the surface states disappear as soon as the distance between the s - and p -defects increases or the sp -coupling decreases.

As a particular example of structure 3 we present in Fig. 4(e) the comparison between calculated transmission coefficients of structure 3 with 4 complete unit cells terminated by the weak bonds (solid line) and the structure with 5 incomplete unit cells (dashed line). As predicted, there is no surface mode for the structure with weak-bond termination [Fig. 2(c), $\eta<1$]. All the eigenvalues get inside of the allowed bands. In agreement with the theory [Fig. 2(d)], one surface mode pointed by arrow in Fig. 4(e) appears close to the middle of the band gap in the structure with incomplete number of unit cells. The field distribution for this mode is very strongly localized to the surface as shown in Fig. 4(g).

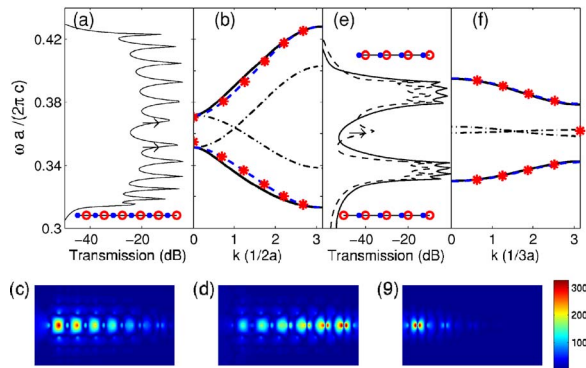


FIG. 4. (Color online) Calculated transmission coefficients for structure 2 (a) and structure 3 (e) in the case of 4 complete unit cells (solid line) and in the case of 5 incomplete unit cells (dashed line), where the arrows indicate the surface modes. The structures are shown in the insets; Spectrum of structure 2 (b) and structure 3 (f) with 5 incomplete unit cells: The two dash-dotted lines show the spectrum of the uncoupled chains of the s - and p -defects. The solid and dashed lines represent the super-cell plane wave calculation and fitted dispersion relation $\omega_{1,2}(k)$ (2) for the infinite chain, respectively. The stars show the calculated spectrum of the finite chain. (c), (d), and (g) show the $|E_z|$ of the surface modes indicated by arrows in (a) and (e), respectively.

We analyze the results of the FDTD simulation in terms of the tight-binding model of Eqs. (1) and (3). First, we found the unknown parameters, $\alpha_{s,p}$, $\beta_{s,p}$, and $\beta_{sp,ps}$, by fitting the dispersion relation $\omega_{1,2}(k)$ (2) to the exact spectrum of the infinite chain calculated using the super-cell plane-wave technique. Using the parameters we calculated the spectrum of the finite chain. The results of our analysis are summarized in Fig. 4(b) for structure 2 with 6 complete unit cells, and in Fig. 4(f) for structure 3 with 5 incomplete unit cells. The two dash-dotted curves that intersect show the spectrum of the uncoupled chains of the s - and p -defects ($\beta_{sp,ps}=0$), respectively. The solid and dashed lines represent the super-cell plane wave calculation and fitted dispersion

relation (2) for the infinite chain, respectively. The stars show the calculated spectrum of the finite chain. The theoretical analysis clearly demonstrates the two surface states close to the band-edge in the case of structure 2 [Fig. 4(b)] and the one surface states in the middle of the band gap in the case of structure 3 with 5 incomplete unit cells [Fig. 4(f)]. The comparison of the FDTD results with the theoretical calculation shows a reasonable agreement between the calculated spectrum of the finite chain [stars in Fig. 4(b) and in Fig. 4(f)] and resonant peaks in the transmission coefficient [Figs. 4(a) and 4(e)].

In conclusion, we demonstrated theoretically and numerically the existence of the Shockley surface states in PCs for the first time. We showed that the Shockley surface states can appear in the PC with either alternating defects supporting the so-called s and p -modes or/and alternating strong and weak bonds. We showed that the Shockley states appear even without any perturbation at the surface ($\alpha'=\alpha$). This is in contrast to the Tamm surface states in PCs which are a direct consequence of the strong surface perturbation, leading to an asymmetry at surfaces ($|\alpha'-\alpha|/\beta>1$). We showed that, similar to the solids, the main feature of the Shockley surface states in PCs is their emergence from the crossing bands. Our study shows that the properties of surface states such as frequency and localization depth can be controlled by coupling parameters and asymmetric parameter. This offers a significant advantage over surface states in other system where one has to accept what ever nature leaves with us. By contrast, surface states can be created or engineered at a desired frequency with specified extent of localization completely by design. Finally, our results will hopefully resolve some of the confusion in the literature regarding the nature of the surface modes and help more fully understand the surface modes in PCs. We believe that the design flexibility coupled with the fuller understanding will eventually benefit the full exploitation of surface states in PCs for many applications including the sub-wavelength optics.

*Electronic address: nmalkova@mail.arc.nasa.gov

†Electronic address: cning@mail.arc.nasa.gov

- ¹P. Yeh, A. Yariv, and C.-S. Hong, *J. Opt. Soc. Am.* **67**, 423 (1977).
- ²H. Raether, *Surface plasmons* (Springer-Verlag, Berlin Heidelberg, 1988); D. L. Mills and E. Burstein, *Rep. Prog. Phys.* **37**, 817 (1974).
- ³W. M. Robertson and M. S. May, *Appl. Phys. Lett.* **74**, 1800 (1999).
- ⁴J. A. Arnaud and A. A. M. Saleh, *Appl. Opt.* **13**, 2324 (1974).
- ⁵P. Yeh and A. Yariv, *Appl. Phys. Lett.* **32**, 104 (1978).
- ⁶R. D. Meade, K. D. Brommer, A. M. Rappe, and J. D. Joannopoulos, *Phys. Rev. B* **44**, R10961 (1991).
- ⁷W. M. Robertson, G. Arjavalingam, R. D. Meade, K. D. Brommer, A. M. Rappe, and J. D. Joannopoulos, *Opt. Lett.* **18**, 528 (1993).
- ⁸J. M. Elson and P. Tran, *Phys. Rev. B* **54**, 1711 (1996).
- ⁹F. Ramos-Mendieta and P. Halevi, *Phys. Rev. B* **59**, 15112

- (1999).
- ¹⁰H. J. Lezec, A. Degiron, E. Devaux, R. A. Linke, L. Martin-Moreno, F. J. Garcia-Vidal, and T. W. Ebbesen, *Science* **297**, 820 (2002).
- ¹¹P. Kramper, M. Agio, C. M. Soukoulis, A. Birner, F. Muller, R. B. Wehrspohn, U. Gosele, and V. Sandoghdar, *Phys. Rev. Lett.* **92**, 113903 (2004).
- ¹²I. E. Tamm, *Phys. Z. Sowjetunion* **1**, 733 (1933); *Z. Phys.* **76**, 849 (1932).
- ¹³W. Shockley, *Phys. Rev.* **56**, 317 (1939).
- ¹⁴S. Enoch, E. Popov, and N. Bonod, *Phys. Rev. B* **72**, 155101 (2005).
- ¹⁵A. Many, Y. Goldstein, and N. B. Grover, *Semiconductor surfaces* (North-Holland, Amsterdam, 1965).
- ¹⁶A. L. Reynolds, U. Peschel, F. Lederer, P. J. Robertson, T. F. Krauss, and P. J. I. de Maagt, *IEEE Trans. Microwave Theory Tech.* **49**, 1860 (2001).
- ¹⁷N. Malkova and C. Z. Ning, *Phys. Rev. B* (to be published).